PNAS
www.pnas.org

Supplementary Materials for

**Metatranscriptomics captures dynamic shifts in mycorrhizal coordination in boreal forests**

S. R. Law[1], A. R. Serrano[1], Yohann Daguerre[1], J. Sundh[2], A. N. Schneider[3], Z. R. Stangl[1,4], D. Castro [1], M. Grabherr[5], T. Näsholm[4], N. R. Street[3]* and V. Hurry*

Correspondence to:
vaughan.hurry@slu.se
nathaniel.street@umu.se

**This PDF file includes:**

**Materials and Methods**

Samples were collected at the Flakaliden research site (64°07′N, 19°27′E, altitude 310–320 m) in the boreal forests of northern Sweden [for details of the site, please refer to Haas et al. (1)]. Treatment of designated experimental plots within the forest stand of an optimal nutrient solution of macro- and micronutrients, including N, P, K, Mg, Ca, S, Fe, B, Mn, Cu and Zn commenced in 1987, and was updated yearly based on analysis of the foliar nutrient status at the site (2). Five root sample replicates were harvested from a single NL plot and a single NE plot (Fig. S1A: plots 6A and 7A, respectively) at each time point during 19 weeks over the 2011 growing season (May to October). Root samples were harvested from 0-25 cm deep soil, cleaned, frozen, and ground. RNA was isolated from 75 mg of tissue using the Ambion™ Plant RNA Isolation Aid and the Ambion™ RNAqueous® kit, followed by a DNA-*free*™ kit DNase treatment. RNA concentration was determined using a Nanodrop™ NL100 and RNA quality was assessed using an Agilent 2100 Bioanalyzer. Using these measurements, the three optimal RNA sample replicates from each treatment/time-point were selected and prepared for RNA sequencing using Illumina TruSeq Stranded mRNA followed by polyA selection. RNA sequencing was performed on a HiSeq2500 at the Science for Life laboratory (Stockholm, Sweden) and 114 transcriptomes were generated (2 treatments x 1 replicate plot x 3 samples in each replicate plot x 19 seasonal sampling points), with a maximum read count of 39 009 534; minimum read count of 2 188 278; and a median read count of 20 060 844. The RNA-Seq raw data is publicly available in the European nucleotide archive (ENA) with the accession PRJEB35805 (3). In 2012, three sample replicates were harvested from each of three replicate NL plots and three replicate NE plots (Fig. S1A: plots 4A, 6A, and 14A; and 1A, 7A, 13A, respectively), at four time points over the 2012 growing season. For these samples, DNA and RNA was isolated. The ITS1 amplicon sequencing data generated from these samples were published previously (1) and reanalyzed by (4). RNA extracted from these Norway spruce root samples was sequenced as described above. 72 transcriptomes were generated (2 treatments x 3 replicate plots x 3 samples in each replicate plot x 4 seasonal sampling points), with a maximum read count of 57 171 651; minimum read count of 2 922 371; and a median read count of 15 672 238. This low temporal resolution collection was used to validate the high temporal resolution samples collected in 2011, in reference to (i) year-to-year variation, (ii) inter-plot variation, and (iii) a complimentary ITS amplicon sequencing approach.

Norway spruce RNA-seq data was pre-processed and aligned with SortmeRNA (5), Trimmomatic (6) and Salmon (7). Pre-processing and analysis of metatranscriptomic data was implemented in a reproducible snakemake workflow available on Bitbucket (https://bitbucket.org/scilifelab-lts/n_street_1801/). A detailed description of software, including parameters and versions used in the workflow, has been published in a separate article (4). Briefly, raw reads were trimmed and quality filtered, fungal reads were then selected and assembled. Assembled fungal transcripts were assigned taxonomic annotation based on sequence similarity to available reference genomes, with ≥85% similarity required for species assignment, ≥60% similarity for genus assignment, and ≥45% for phylum assignment (8, 9). If a similarity threshold to a given

taxonomic level was not satisfied, the prefix 'Unclassified' was assigned before the next highest classification, e.g. "Unclassified Cortinarius" indicates similarity to the available reference genome was >60% but <85%. Functional annotations were assigned using eggnog-mapper (10) and the eggNOG database. For both Norway spruce and fungi, high dimensional data analysis was performed using PCA and extended with PHATE (11). Differential expression analysis and variance stabilization transformation were carried out with DESeq2 (12). Co-expression networks were constructed using Seidr (13) and clustered using Infomap (14). Seidr is an open-source toolkit the uses a number of published algorithms for inferring gene expression networks. For each possible edge in the network the highest scoring edge across the included algorithms is selected and a consensus, aggregated network is produced. Tools included in seidr, again implemented from published algorithms, are then used to remove edges most likely to represent noise. Co-expression networks were generated for individual species of interest (e.g. Norway spruce, *Piloderma olivaceum*, *Cenococcum geophilum*, etc.), within which similarly expressed genes were grouped into Network Modules. For each Network Module an eigengene was created, representing the 1st principal component of all the genes within that Network Module—providing a unified and scale-free expression profile representative of all the genes in that particular Network Module. Next, rather than comparing the expression of individual fungal or tree genes (as would be conventional), we calculated correlations using the Network Module eigengene expression profiles to identify modules in the two networks with correlated seasonal profiles. Gene enrichment tests were carried out with Gofer3, an in-house tool at the Umeå Plant Science Centre (DOI:10.5281/zenodo.3731544). All enrichment tests can be accessed on the BRA web app (https://www.boreal-atlas.info/). All other analyses were executed using in-house tools. All scripts are available on Github (https://github.com/loalon/flakaliden-2011).

**Supplementary Text**

*The boreal forest as a site for investigating the effect of nutrient enrichment on root-associated fungal communities*

Samples were collected at the Flakaliden research site (64°07′N, 19°27′E, altitude 310–320 m) in the boreal forests of northern Sweden [for details of the site, please refer to Haas et al. (1)]. Boreal forests girdle the terrestrial environments of the northern latitudes, are dominated by coniferous tree species, and comprise the second largest biome in the world. Consequently, they play pivotal roles as wildlife habitats, sites of vast carbon sequestration, and the foundation of many important timber industries across the Northern Hemisphere. These soils are highly nutrient limited, as low annual soil temperatures hinder nutrient mineralization rates and their isolation has shielded them from extensive anthropogenic nutrient deposition. A high-resolution map of the Flakaliden research site is provided in Fig. S1A. Treatment with a balanced nutrient solution of designated experimental plots within the forest stand commenced in 1987. This treatment had a profound effect on tree growth, with trees from fertilized plots on average 4 m taller and with four times the above-ground biomass of trees grown on NL plots (15)( Fig. S1H). Belowground biomass was also greater in trees from fertilized plots but to a lesser extent (16) and the percentage of root tips

colonized by ectomycorrhizal fungi was significantly lower than in low-nutrient grown roots (17). To aid the analysis and interpretation of the Boreal Rhizospheric Atlas, supporting climatic, phenological, and physiological metadata was collated and made available within the corresponding online tool (Fig. S1B-G).

**Supplemental Methods**

*General workflow*

Fig. 1 summarizes the analysis as a whole, on the following sections each main process will be explained with further detail. The scripts using in each step are available in the following repository: https://github.com/loalon/flakaliden-2011

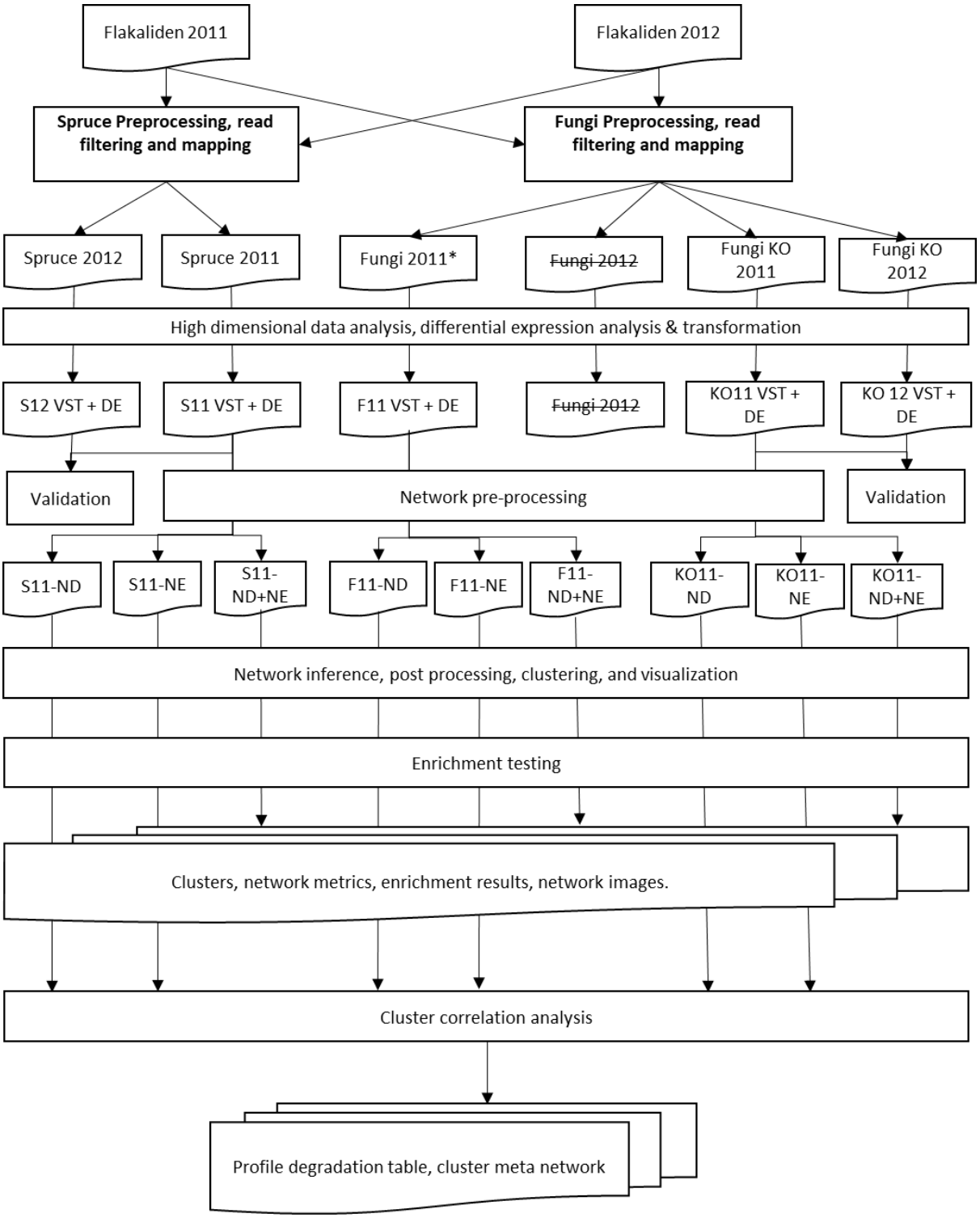
Flakaliden 2011
Flakaliden 2012
Spruce Preprocessing, read filtering and mapping
Fungi Preprocessing, read filtering and mapping
Spruce 2012
Spruce 2011
Fungi 2011*
~~Fungi 2012~~
Fungi KO 2011
Fungi KO 2012
High dimensional data analysis, differential expression analysis & transformation
S12 VST + DE
S11 VST + DE
F11 VST + DE
~~Fungi 2012~~
KO11 VST + DE
KO 12 VST + DE
Validation
Network pre-processing
Validation
S11-ND
S11-NE
S11-ND+NE
F11-ND
F11-NE
F11-ND+NE
KO11-ND
KO11-NE
KO11-ND+NE
Network inference, post processing, clustering, and visualization
Enrichment testing
Clusters, network metrics, enrichment results, network images.
Cluster correlation analysis
Profile degradation table, cluster meta network

*SPRUCE Preprocessing, read filtering, and mapping*

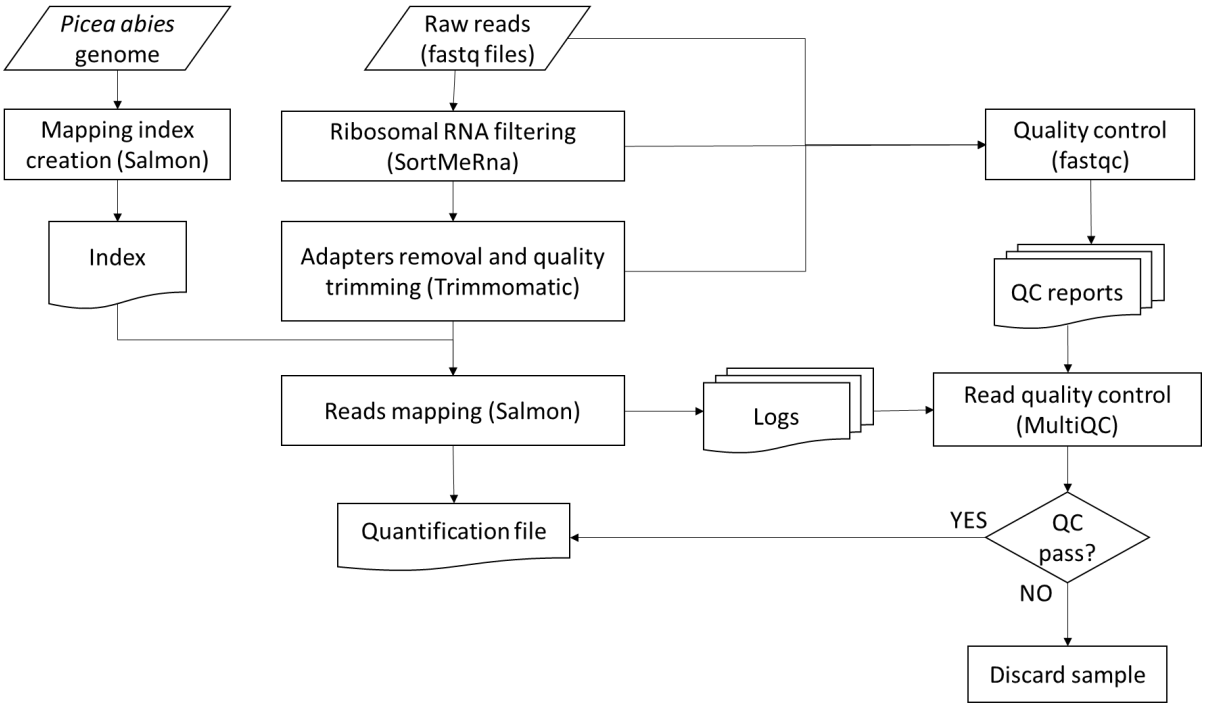


| STEP | NAME | VERSION | PARAMETERS | REF |
|---|---|---|---|---|
| **Ribosomal RNA Filtering** | SortMeRna | 2.1 | --fastx --paired_in --other | [1] |
| **Adapters removal and quality trimming** | Trimmomatic | 0.36 | ILLUMINACLIP:TruSeq3-PE.fa:2:30:10 SLIDING WINDOWS:5:20 MINLEN:50 | [2] |
| **Quality control** | fastqc | 0.11.4 | default | [3] |

| | | | | |
|---|---|---|---|---|
| **Read quality control** | MultiQC | 1.5 | default | [4] |
| **Mapping Index creation** | Salmon | 0.11 | index --type quasi -k 31 | [5] |
| **Mapping-based quantification** | Salmon | 0.11 | quant --libType IU | [5] |

The index used for Salmon mapping is based on the *Picea abies* genome (v1.0) [6]

*Fungi Preprocessing, read filtering and mapping*

Preprocessing and analysis of metatranscriptomic data was implemented in a reproducible snakemake workflow available on Bitbucket (https://bitbucket.org/scilifelab-lts/n_street_1801/). A detailed description of software and parameters used in the workflow has been published in a separate preprint article [7]. Briefly, raw reads were trimmed and filtered, after which fungal reads were selected and assembled. Assembled fungal transcripts were assigned available taxonomic and functional annotation. Taxonomy was assigned to the assembled contigs using the tool contigtax (v. 0.5.7) (21).

*High dimensional data analysis, differential expression analysis & transformation. Network pre-processing*

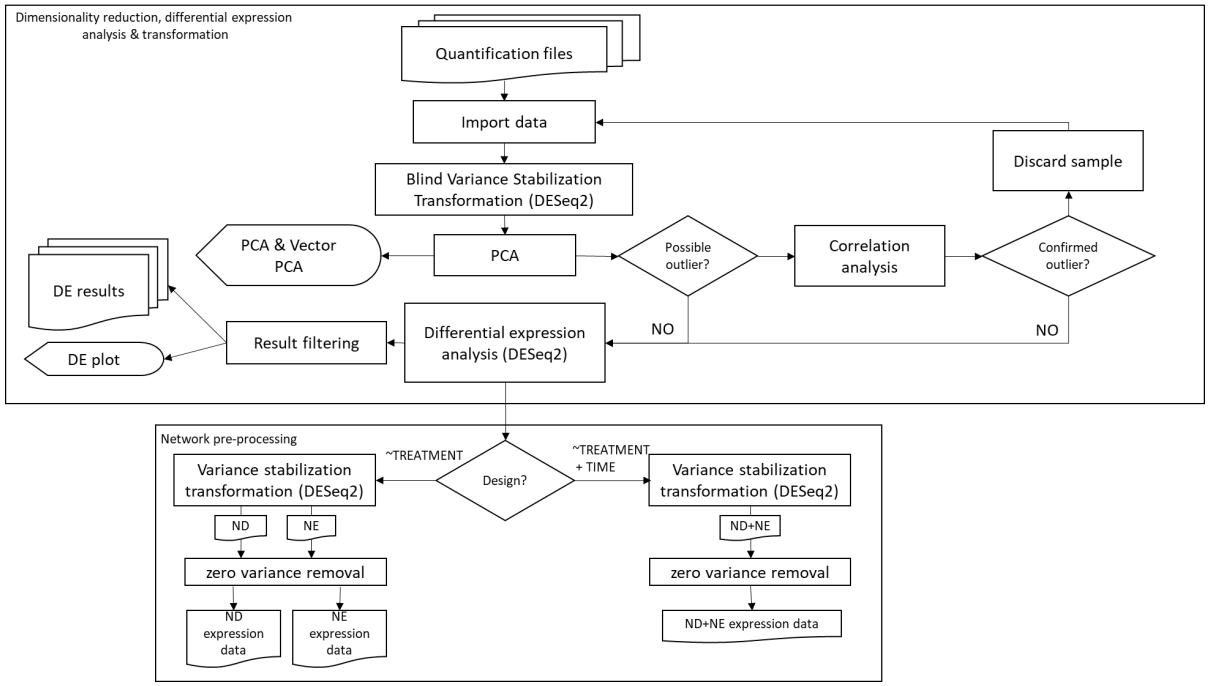

| STEP | NAME | VERSION | PARAMETERS | REF |
|---|---|---|---|---|
| **Blind variance stabilization transformation** | DESeq2 (vst) | 1.24.0 | blind=TRUE | 9 |
| **variance stabilization transformation** | DESeq2 (vst) | 1.24.0 | Blind=FALSE | 9 |
| **Differential expression analysis** | DESeq2 | | | 9 |
| **PCA & Vector PCA** | Rtoolbox | | | 11 |
| **Zero variance removal** | Package matrixStats | 0.56.0 | | |

Result filtering was performed by keeping all genes with a log2 fold change above 0.5 or below 0.5 and a pAdj value below 0.01.

For the 2011 fungal dataset an additional high dimensional analysis was performed using PHATE [10] 1.0.1 with default parameters.

*Network inference, post processing, clustering, and visualization*

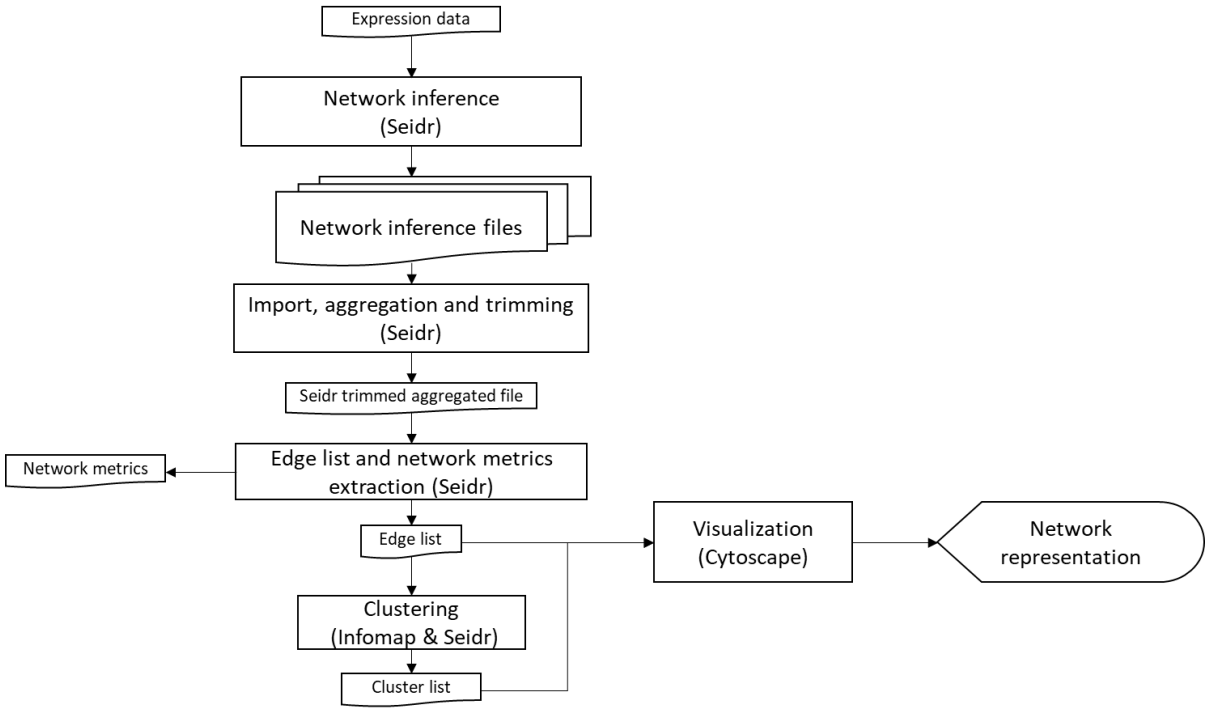


| STEP | NAME | VERSION | PARAMETERS | REF |
|---|---|---|---|---|
| **Network inference** | Seidr inference methods | 0.11.0 | Default parameters for each method. Inference methods used: Arance, Clr, Elnet, Genie3, LLR, Narromi, Pcor, Pearson, Plsnet, Spearman, Tigress | 12 |
| **Import** | Seidr | 0.11.0 | For all inference methods “-z –r –n”<br>Aracne, Clr, Pearson, and Pcor<br>“-lm”. Other methods “-m” | 12 |
| **Aggregate** | | | -m irp | |
| **Trimming** | | | describe -b 100 -q $(seq -s ',' 0.01 0.01 0.99)<br>threshold -n 1000 -m <value> -M 1.0 | |
| **Edge list extraction** | | | view -d $'\t' | |
| **Metrics extraction** | | | stats $1 -m PR,BTW,STR,EV,KTZ<br>view –c –D -d $'\t' | |

| | | | | |
|---|---|---|---|---|
| **clustering** | Infomap | 0.19.26 | -z –Markov-time 1* | 13 |
| **Visualization** | Cytoscape | 3.6.1 | | 14 |

* The specific value of the Markov-time for each network is within the individual report for that network

Three networks were calculated (NL, NE, NL+NE) with the following expression data: spruce, fungal Kegg Orthologs, and with the full fungal data only for the following genera: *Piloderma, Cortinarius, and Cenococcum geophilum*.

The Seidr threshold minimal value was different for each network. The first step to determine this value was to use 'Seidr describe' to obtain a minimal threshold search value. This minimal value is optional but speeds up the search process for determining the optimal threshold value.

'Seidr threshold' generates a table containing the different threshold values, number of nodes and edges, scale free fit and average clustering coefficient value. Using custom R scripts, the threshold value that maximized the average clustering coefficient and number of nodes, while maintaining a scale free fit value higher than 0.9 was obtained.

The network centrality metrics calculated were PageRank, Betweenness, Strength, Eigenvector and Katz.

Infomap (version 0.19.26)(14) requires a network edge list with indices that is generated in the edge list extraction step. Infomap generates a tree file with the results and the granularity of the clustering (levels).

To select a proper clustering level, we used custom R scripts to analyze how many genes were within the 20 biggest clusters. If the number of genes was between 50-60% of all network genes, that level was accepted, otherwise next level was selected and checked. If none of the levels matched these criteria, the Markov time parameter was explored. If there were a high number of modules to match the criteria, the parameter was increased in small increments (0.1), while if the module number was low then the parameter was decreased.

Finally, 'seidr resolve' was used to convert gene indices back to the actual gene names and a final table containing network gene names and module names is obtained.

*Enrichment testing*

This step was carried out using gene enrichment tool gofer3 [15]. After providing a set of genes, a background, a series of enrichment tests and a cut-off value the Gofer3 tool returns a table with the enrichment results and an FDR-adjusted p-value (pAdj). Only enrichments with a pAdj value <0.05 were considered significant. For Norway spruce the following tests were carried out: Gene ontology, Mapman, KEGG enzymes and Pfam. For fungal KEGG orthologues only KEGG pathways were tested. As some KEGG orthologs were annotated to human-related diseases, these terms were renamed as 'miss-annotated'. For fungal species, GO, KEGG, KO, KEGG pathways, COG and KOG tests were carried out.

*Cluster correlation analysis*

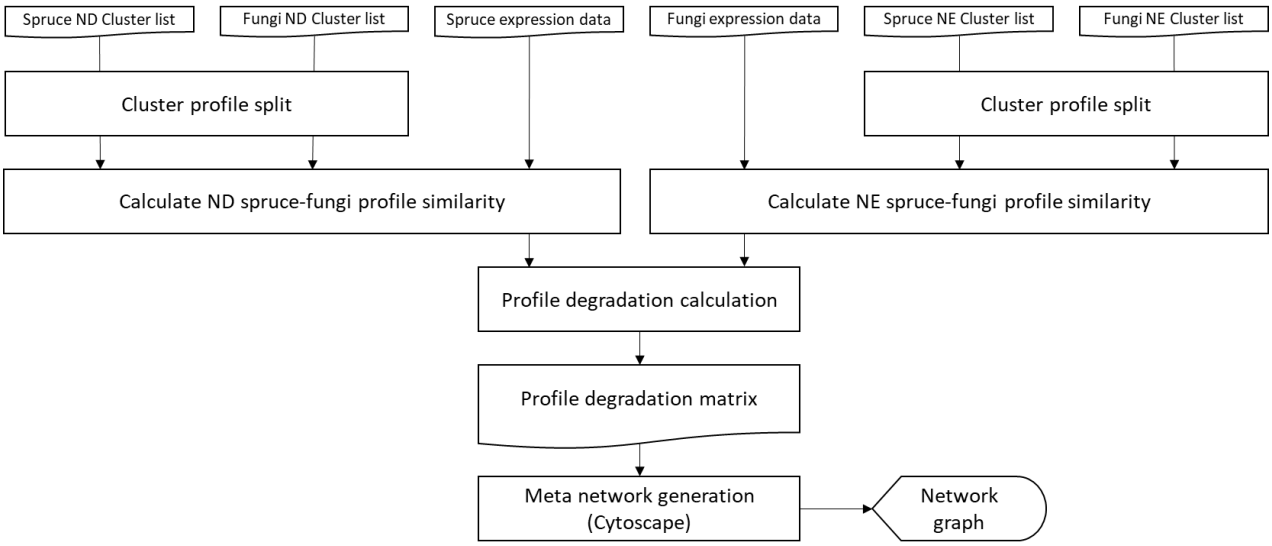


This step begins with a cluster profile split. For each Infomap module obtained in the previous steps, a PCA was carried out with the genes in that module. Then the module was divided into a positive correlation sign module containing all genes with a PCA rotation value higher than 0 and a negative module if the value is lower than 0.

In the NL profile similarity step, a Spearman correlation was executed for the eigengene of every Norway spruce split (positive/negative) module vs every the eigengene of every fungal split module. The result generated a table with all pairwise correlations and their associated correlation value. The same step was also performed using NE network modules.

The profile degradation calculation used the value of each NL pairwise correlation between species and subtracted the value from the NE counterpart. A negative profile degradation value indicated that the correlation between two particular clusters had increased due to the nutrient enrichment treatment, whereas a positive value indicated a reduction in coordination between the modules.

The procedures in these steps were performed using custom scripts. These are collated into an associated repository at https://github.com/loalon/flakaliden-2011. The meta network generation and visualization was performed with Cytoscape v3.6.1 [14].

*Host-microbe coordination analysis*

For the three most abundant fungal genera (*Piloderma*, *Cortinarius*, and *Cenococcum*), host-microbe coordination analysis was carried out at two levels: (i) a broad functional level, using Spearman rank correlation to measure coordination between Network modules of a given fungi and Network Modules of Norway Spruce; and (ii) a fine functional level, using Spearman rank correlation to measure coordination between an individual predicted fungal effector and the complete Norway Spruce transcriptome. In both cases, to be considered "coordinated" the correlation between two Network Modules or between a fungal effector and a Norway spruce transcript had to satisfy the following: $r_s$ (> 0.7 or <-0.7) and adjusted p-value thresholds (<0.001). This was carried out in NL and NE conditions in isolation, to establish if coordination was observed in NL, NE, or BOTH conditions. Functional enrichment of Norway spruce and fungal Network Modules, as well as Norway spruce transcripts coordinated with individual fungal effectors was carried out using the Boreal Rhizospheric Atlas online tool.

*Prediction of candidate fungal effectors*

The following was carried out for all identified sequencing reads of the three most abundant fungal genera (*Piloderma*, *Cortinarius*, and *Cenococcum*). First, to identify genes encoding putative secreted proteins, amino acid sequences of all transcripts were assessed for the presence of signal peptides using SignalP 5.0 (18) and Phobius (19) predictive toolsets. All transcripts predicted to be secreted by at least one of these predictive tools were then further assessed using the EffectorP machine learning method for fungal and oomycete effector prediction in secretomes (20). EffectorP versions 1.0 and 2.0 were employed for this analysis.

## Table S1. List of predicted fungal effectors of *Cortinarius glaucopus*, *Piloderma olivaceum* and Cenococcum geophilum

| Species | Gene ID | Homology to known protein(s) | Predicted domain(s) | Putative functions | Predicted plant subcellular localization(s) |
|---|---|---|---|---|---|
| *Cortinarius glaucopus* | Cgla107037 | Tim17-domain-containing protein [*Cortinarius glaucopus*] | TIM23 (Panther) | Protein import | - |
| | Cgla197435 | - | - | - | - |
| | Cgla234290 | hypothetical protein [*Cortinarius glaucopus*] | - | - | Chloroplast |
| | Cgla281293 | - | - | - | - |
| | Cgla281448 | hypothetical protein [*Cortinarius glaucopus*] | - | - | - |
| | Cgla286380 | DWNN-domain-containing protein [*Cortinarius glaucopus*] | - | - | - |
| | Cgla314063 | hypothetical protein [*Cortinarius glaucopus*] / vitamin-D-receptor interacting mediator subunit 4-domain-containing protein [*Crassisporium funariophilum*] | Mediator complex, subunit Med4 (InterPro) | Mediator complex (middle module) | - |
| | Cgla320161 | DUF974-domain-containing protein [*Cortinarius glaucopus*] / Trafficking protein particle complex subunit 13 | Trafficking protein particle complex subunit 13 (InterPro) | Vesicle trafficking | Chloroplast |
| *Piloderma olivaceum* | Poli103921 | hypothetical protein [*Piloderma croceum*] / Phosphatidylglycerol/phosphatidylinositol transfer protein | Sterol transport protein NPC2-like (InterPro) | Sterol transport | - |
| | Poli12446 | hypothetical protein [*Piloderma croceum*] | - | - | - |
| | Poli13284 | hypothetical protein [*Piloderma croceum*] | - | - | - |
| | Poli134967 | hypothetical protein [*Piloderma croceum*] / cytochrome b5-like heme/steroid binding domain-containing protein | Cyt B5-like heme/steroid-binding (InterPro) | Electron transport/metal binding | - |
| | Poli146008 | hypothetical protein [*Piloderma croceum*] | - | - | - |
| | Poli148183 | hypothetical protein [*Piloderma croceum*] / acyl-CoA N-acyltransferase [*Boletus edulis*] | GNAT domain + Acyl CoA acyltransferase (InterPro) | Sugar/fatty acid metabolism | Nucleus |
| | Poli157229 | hypothetical protein [*Piloderma croceum*] / Tim17-domain-containing protein [*Suillus decipiens*] | Mitochondrial import inner membrane translocase subunit TIM22 (InterPro) | Protein import | - |
| | Poli165314 | hypothetical protein [*Piloderma croceum*] / Dynactin subunit 2 [*Hypsizygus marmoreus*] | Intrinsic Disorder (mobidb-lite) | - | Nucleus |
| | Poli167869 | hypothetical protein [*Piloderma croceum*] / NAD(P)-binding protein [*Crucibulum laeve*] | Short-chain dehydrogenase/reductase SDR (InterPro) | Oxidoreductase activity | Nucleus |
| | Poli171134 | hypothetical protein [*Piloderma croceum*] / cwf21-domain-containing protein [*Fibularhizoctonia* sp.] | Serine/arginine repetitive matrix 2 (Panther) | mRNA splicing | Nucleus |
| | Poli171530 | hypothetical protein [*Piloderma croceum*] / FAD/NAD-binding domain-containing protein [*Rickenella mellea*] | FAD/NAD(P)-binding domain superfamily | Oxidoreductase activity | Mitochondria + Nucleus |
| | Poli171550 | hypothetical protein [*Piloderma croceum*] / DnaJ-domain-containing protein [*Fibularhizoctonia* sp.] | DnaJ domain (InterPro) | Protein folding | - |
| | Poli179170 | hypothetical protein [*Piloderma croceum*] / putative calnexin [*Mycena venus*] | Calreticulin/calnexin (InterPro) + calnexin 14D-related (Panther) | Calcium binding/protein folding | Nucleus |
| | Poli196148 | hypothetical protein [*Piloderma croceum*] / pyruvate dehydrogenase e1 component beta subunit [*Suillus decipiens*] | Pyruvate dehydrogenase E1 component + Transketolase-like Pyr-bd (InterPro) | Pyruvate dehydrogenase activity | - |
| | Poli223006 | hypothetical protein [*Piloderma croceum*] / Threonyl-tRNA synthetase [*Fibularhizoctonia* sp.] | Threonine-tRNA ligase, class Iia (InterPro) | tRNA aminoacylation | - |
| | Poli235293 | hypothetical protein [*Piloderma croceum*] / Dabb family protein [*Microbacterium rhizomatis*] | Stress-response A/B barrel domain-containing protein HS1/DABB1-like (ProSite) | - | - |
| | Poli237743 | hypothetical protein [*Piloderma croceum*] | Intrinsic Disorder (mobidb-lite) | - | Nucleus |
| | Poli241503 | hypothetical protein [*Piloderma croceum*]/transmembrane adaptor Erv26-domain-containing protein [*Suillus clintonianus*] | Svp26/Tex261 (InterPro) | Vesicle trafficking | Mitochondria |
| | Poli242590 | hypothetical protein [*Piloderma croceum*] | Peptidyl-prolyl cis-trans isomerase FKBP2/11 (InterPro) | Protein folding | Nucleus |
| | Poli245894 | hypothetical protein [*Piloderma croceum*] / N-terminal nucleophile aminohydrolase [*Fibularhizoctonia* sp.] | Proteasome subunit beta 5 (InterPro) | Protein degradation | - |
| | Poli249960 | hypothetical protein [*Piloderma croceum*] / MSF1-domain-containing protein [*Fibularhizoctonia* sp.] | Slowmo/Ups family +PRELI domain (InterPro) | Phospholipid metabolism | - |
| | Poli256117 | hypothetical protein [*Piloderma croceum*] | Osmotin/thaumatin-like sf (InterPro) | Antibiotic activity | - |
| | Poli257735 | hypothetical protein [*Piloderma croceum*] | - | - | - |
| | Poli265379 | hypothetical protein [*Piloderma croceum*] | Protein kinase domain + Tyr kinase active site (InterPro) | Protein phosphorylation activity | - |
| | Poli275986 | - | - | - | - |
| | Poli312055 | hypothetical protein [*Piloderma croceum*] | - | - | - |
| | Poli312783 | hypothetical protein [*Piloderma croceum*] / acyl- thioester [*Moniliophthora roreri*] | - | - | - |
| | Poli48819 | - | Tyr phosphatase dual domain (InterPro) | Protein dephosphorylation activity | - |
| | Poli60822 | hypothetical protein [*Piloderma croceum*] / NAD(P)-binding protein [*Fibularhizoctonia* sp.] | UDP-glucuronic acid decarboxylase (InterPro) | D-xylose metabolism | - |
| | Poli62948 | hypothetical protein [*Piloderma croceum*] / acetyl-CoA synthetase-like protein [*Fibularhizoctonia* sp.] | - | Acetyl-CoA synthesis | - |
| | Poli84736 | hypothetical protein [*Piloderma croceum*] / Cyclin-like protein [*Mycena venus*] | Cyclin/Cyclin-like subunit Ssn8 (InterPro) | Mediator complex (kinase module) | Mitochondria |
| | Poli85888 | hypothetical protein [*Piloderma croceum*] | Zn(2)-C6 fungal-type DNA-binding domain (InterPro) | Transcriptional regulation | Nucleus |
| | Poli95862 | hypothetical protein [*Piloderma croceum*] / Acetyl-CoA acetyltransferase B, mitochondrial [*Grifola frondosa*] | Mitochondrial acetyl-CoA acetyltransferase (InterPro) | Acetyl-CoA biosynthesis | - |
| *Cenococcum geophilum* | Cgeo120948 | hypothetical protein [*Cenococcum geophilum*] / fungal-specific transcription factor domain-domain-containing protein [*Clohesyomyces aquaticus*] | Intrinsic Disorder (mobidb-lite) | - | Nucleus |
| | Cgeo145501 | hypothetical protein [*Cenococcum geophilum*] | Intrinsic Disorder (mobidb-lite) | - | - |
| | Cgeo15314 | AMP-binding enzyme [*Cenococcum geophilum*] | Acetyl-CoA synthetase-like (SSF) + AMP-binding C (Pfam) | Acetyl-CoA biosynthesis | - |
| | Cgeo160874 | hypothetical protein [*Cenococcum geophilum*] | Hyphal anastamosis-8 protein (Panther) + Intrinsic Disorder (mobidb-lite) | Hyphal fusion | - |
| | Cgeo192012 | hypothetical protein [*Byssothecium circinans*] / WSC domain-containing protein [*Pyrenophora tritici-repentis*] | - | Carbohydrate binding | Nucleus |
| | Cgeo203209 | hypothetical protein [*Cenococcum geophilum*] | Intrinsic Disorder (mobidb-lite) | - | Nucleus |
| | Cgeo220123 | hypothetical protein [*Glonium stellatum*] | Intrinsic Disorder (mobidb-lite) | - | Chloroplast |
| | Cgeo220791 | TFIID-18kDa-domain-containing protein [*Cenococcum geophilum*] | Transcription initiation factor IID, subunit 13 +Histone-fold (InterPro) | General transcription factor | Nucleus |
| | Cgeo225177 | hypothetical protein [*Glonium stellatum*] / phd finger containing phf1 [*Pyrenophora seminiperda*] | Intrinsic Disorder (mobidb-lite) | - | Chloroplast |
| | Cgeo24592 | MAGE-domain-containing protein [*Cenococcum geophilum*] | Melanoma-associated antigen MAGE (InterPro) | - | Nucleus |
| | Cgeo28170 | hypothetical protein [*Cenococcum geophilum*] | - | - | - |
| | Cgeo286913 | hypothetical protein [*Cenococcum geophilum*] / bZIP transcription factor-like protein [*Polyplosphaeria fusca*] | bZIP (InterPro) + Leucine zipper domain (SSF) +Intrinsic Disorder (mobidb-lite) | Transcriptional regulation | Nucleus |
| | Cgeo292715 | RmlC-like cupin [*Cenococcum geophilum*] | Pirin N (InterPro) | - | Chloroplast + Mitochondria |
| | Cgeo295335 | cell division control protein 3/GTP binding protein [*Cenococcum geophilum*] / Septin [*Lepidopterella palustris*] | Intrinsic Disorder (mobidb-lite) | - | - |
| | Cgeo31273 | hypothetical protein [*Cenococcum geophilum*] / gpi anchored serine-rich protein [*Fusarium circinatum*] | - | - | - |
| | Cgeo4216 | hypothetical protein [*Cenococcum geophilum*] | - | - | - |
| | Cgeo48188 | - | Intrinsic Disorder (mobidb-lite) | - | Chloroplast + Mitochondria + Nucleus |
| | Cgeo49785 | hypothetical protein [*Cenococcum geophilum*] | - | - | - |
| | Cgeo51667 | hypothetical protein [*Cenococcum geophilum*] / EthD domain-containing protein [*Massariosphaeria phaeospora*] | EthD domain (InterPro) | Pigment production | Mitochondria + Nucleus |
| | Cgeo64882 | hypothetical protein [*Cenococcum geophilum*] / Zinc finger C2H2-type protein [*Macrophomina phaseolina*] | Intrinsic Disorder (mobidb-lite) | - | Chloroplast |
| | Cgeo73057 | hypothetical protein [*Cenococcum geophilum*] | Intrinsic Disorder (mobidb-lite) | - | - |
| | Cgeo8505 | hypothetical protein [*Cenococcum geophilum*] / UBC-like protein [*Glonium stellatum*] | Ubiquitin-conjugating enzyme E2 (InterPro) | Ubiquitinylation | - |
| | Cgeo89483 | S-adenosyl-L-methionine-dependent methyltransferase [*Cenococcum geophilum*] | Probable tRNA methyltransferase 9-like protein (InterPro) | tRNA wobble uridine modification | Nucleus |

**Supplementary Figures:**

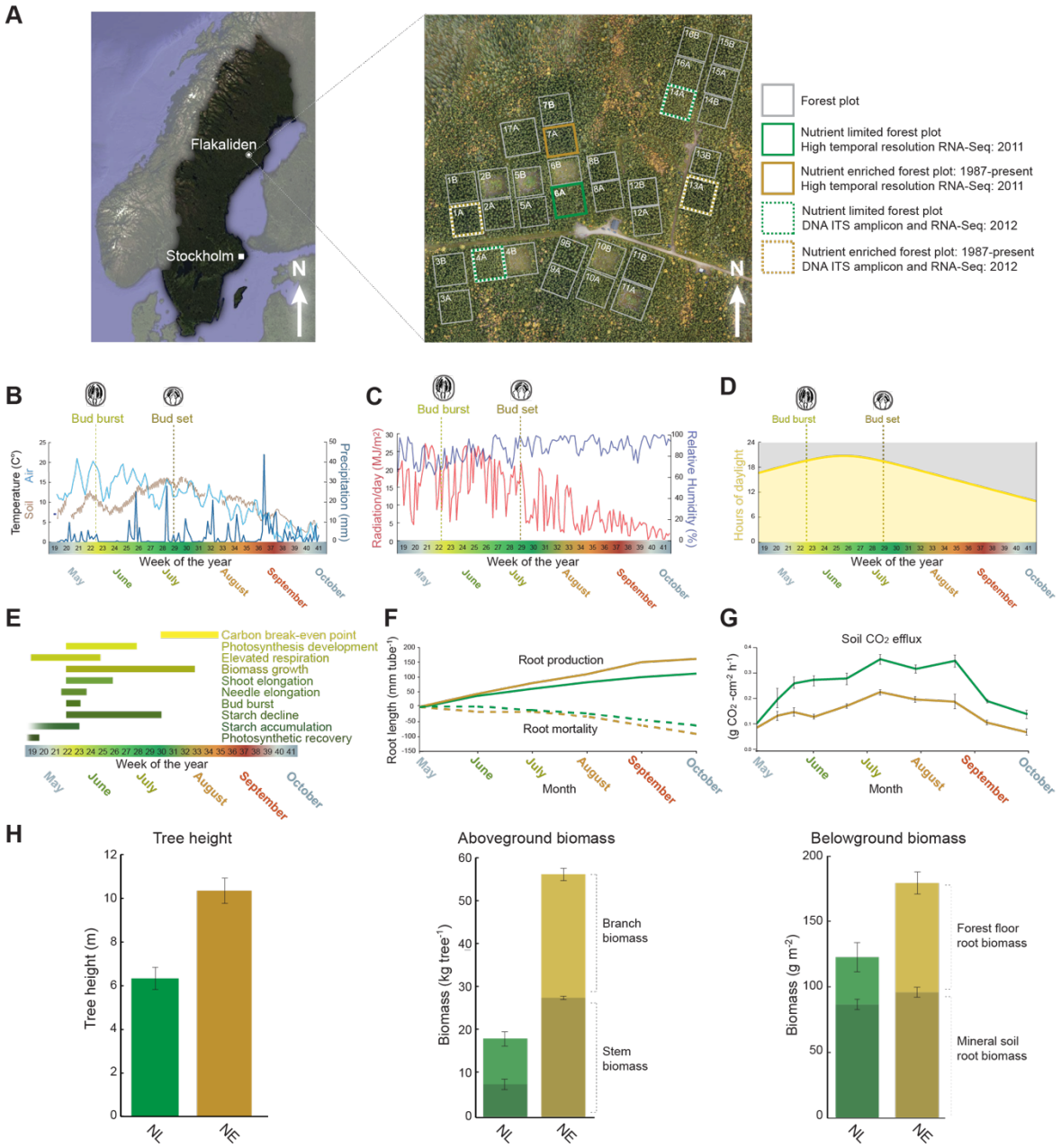


**Fig. S1. Climatic and phenological metadata for the Flakaliden research site in 2011 (64°07′N, 19°27′E, altitude 310–320 m). (A)** Location and layout of the Flakaliden research site. **(B)** Air and soil temperature (soil temperatures recorded at Svartberget field research station (64°14′N, 19°34′E), in 2011), and precipitation recorded at Flakaliden in 2011. **(C)** Radiation and relative humidity recorded at Flakaliden in 2011. **(D)** Day length at Flakaliden in 2011. **(E)** Phenological milestones of Norway spruce grown at Flakaliden. Modified from (21) **(F)** Cumulative length production and mortality of spruce roots (mm $tube^{-1}$) in the mineral soil layer at Flakaliden. A green line indicates nutrient limited soil; a gold line indicates nutrient enriched soil. Modified from (16). **(G)** Soil $CO_2$ efflux ($gCO_2$ $cm^{-2}$ $h^{-1}$) at Flakaliden. A green line indicates

nutrient limited soil; a gold line indicates nutrient enriched soil. Modified from (22). **(H)** Tree height (m), aboveground biomass (kg $tree^{-1}$) and belowground biomass (g $m^{-2}$) of nutrient limited and nutrient enriched Norway spruce (15, 16).

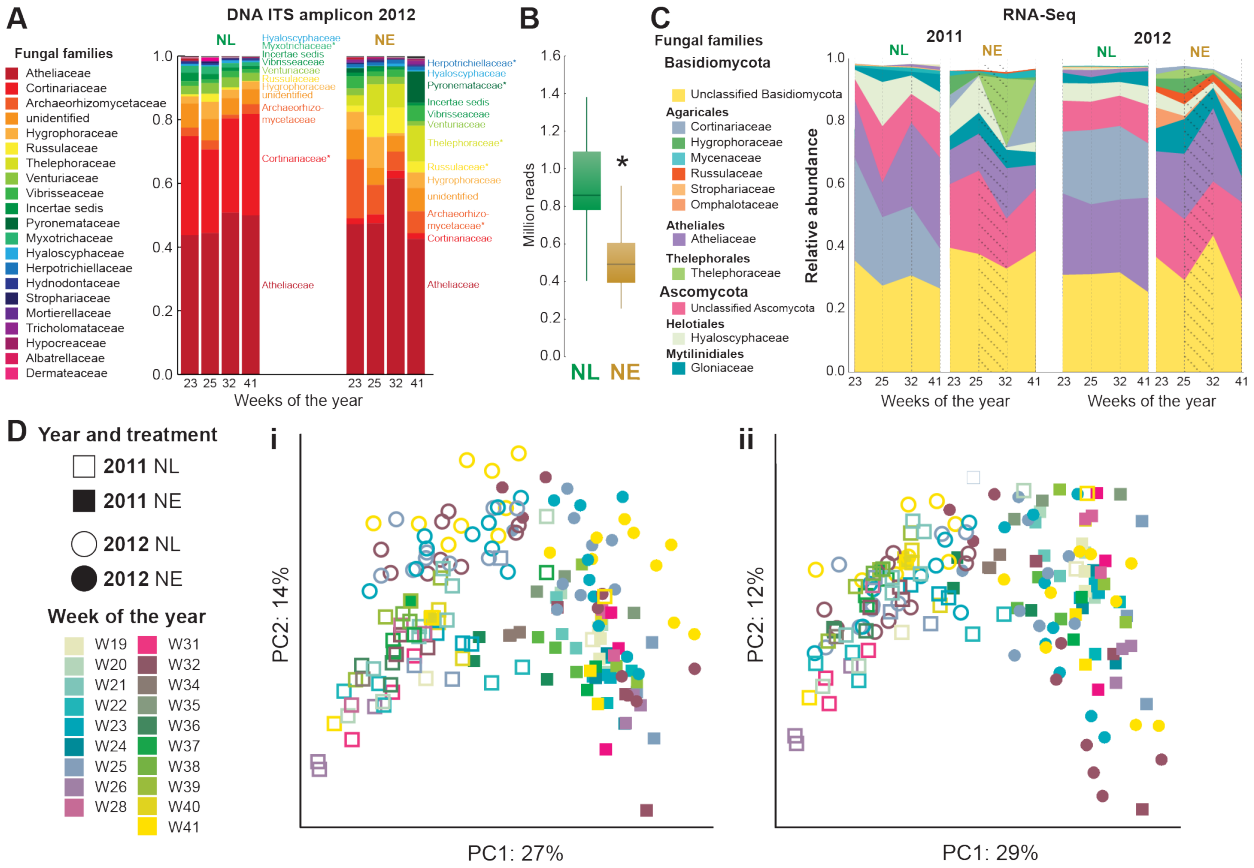


**Fig. S2. Comparison of root-associated fungal community metagenomes and metatranscriptomes from nutrient limited and nutrient enriched forest plots over the growing seasons of 2011 and 2012.** In addition to the high temporal resolution RNA-Seq experiment carried out in 2011, samples were collected in 2012 at a lower temporal resolution (four time points across the season versus nineteen in 2011), but in three experimental forest plots per treatment (six in total). DNA ITS amplicon sequencing and RNA-Seq were performed on these samples and the results were used to validate the observations made in 2011. **(A)** The number of ITS1 reads assigned to the 21 most abundant fungal families was normalized to the total number of ITS1 reads and plotted across the sampling time course for both NL and NE conditions in 2012. **(B)** Distribution of fungal RNA-Seq reads observed per time point in NL and NE conditions in 2012. An * indicates significant difference between NL and NE ($P$<0.001; two-tailed Wilcoxon Signed-Rank Test) **(C)** For 2011 and 2012, the number of RNA-Seq reads assigned to each fungal family was normalized to the total number of fungal reads present in a given sampling-year and the top 10 most abundant fungal families in each treatment identified (12 families in total). The normalized read count of these 10 families were plotted across the sampling time courses for both NL and NE (to increase comparability, the plot from 2011 has been modified from Fig. 1C to match the time points collected in 2012). The period of nutrient enrichment (June to August) is indicated by a shaded box. **(Di)** PCA of KEGG orthologues of root-associated fungal metatranscriptomes from sampling time courses for both NL and NE conditions in both 2011 and 2012, and **(Dii)** when year-effect has been removed.

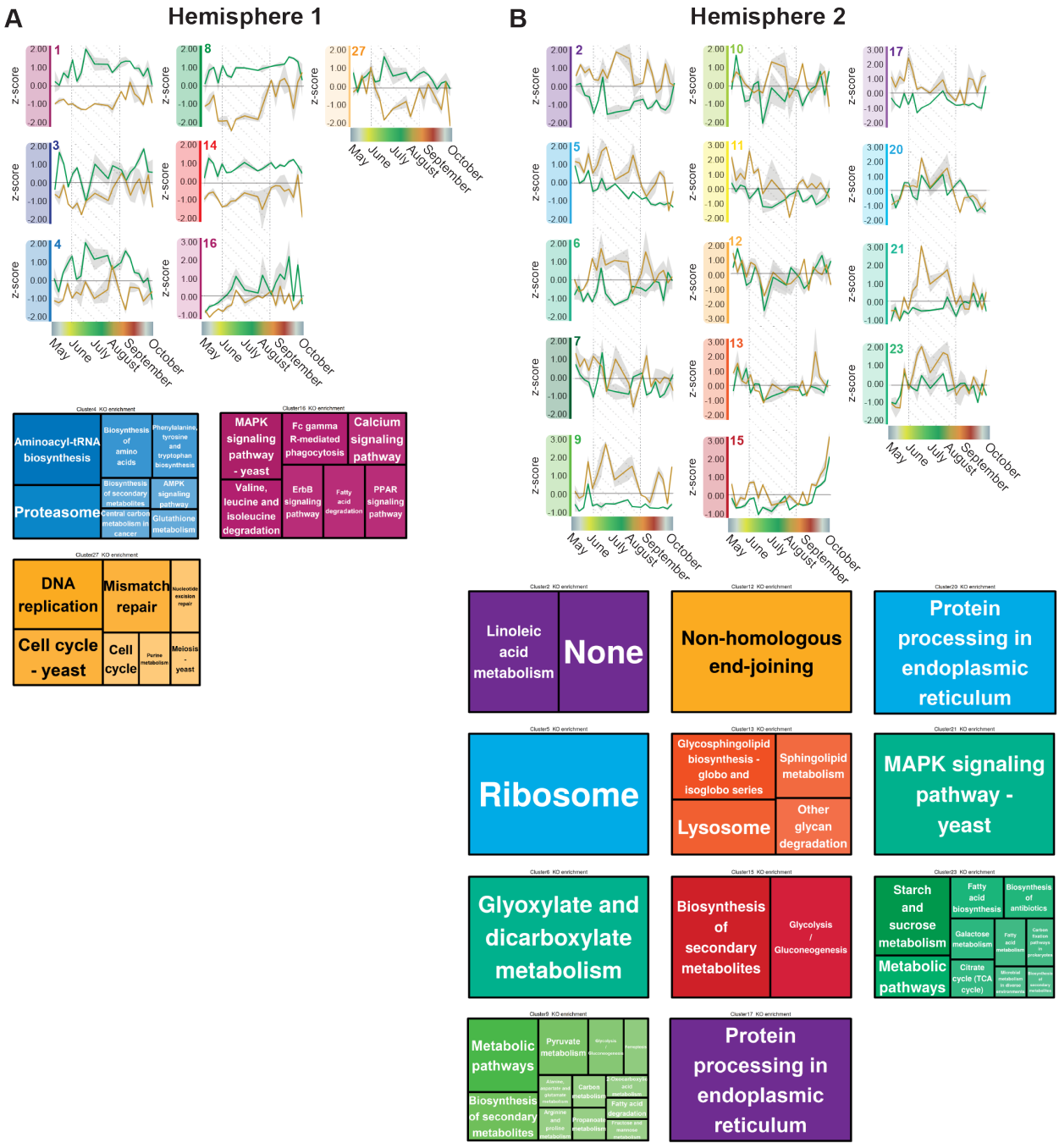


**Fig. S3. Functional analysis of a co-expression network of a root-associated fungal community metatranscriptome, from nutrient limited and nutrient enriched samples over a growing season.** The metatranscriptomic co-expression network was clustered into 27 network modules, and the 21 largest of these was analyzed for functional enrichment. For the genes comprising the network modules of **(A)** Hemisphere 1 and **(B)** Hemisphere 2, treemaps of significantly enriched functional categories have been listed (adjusted $P$<0.05 in all cases; Fisher exact test). Where functional categories have not been listed for the genes comprising a network module, no significant functional enrichment was found.

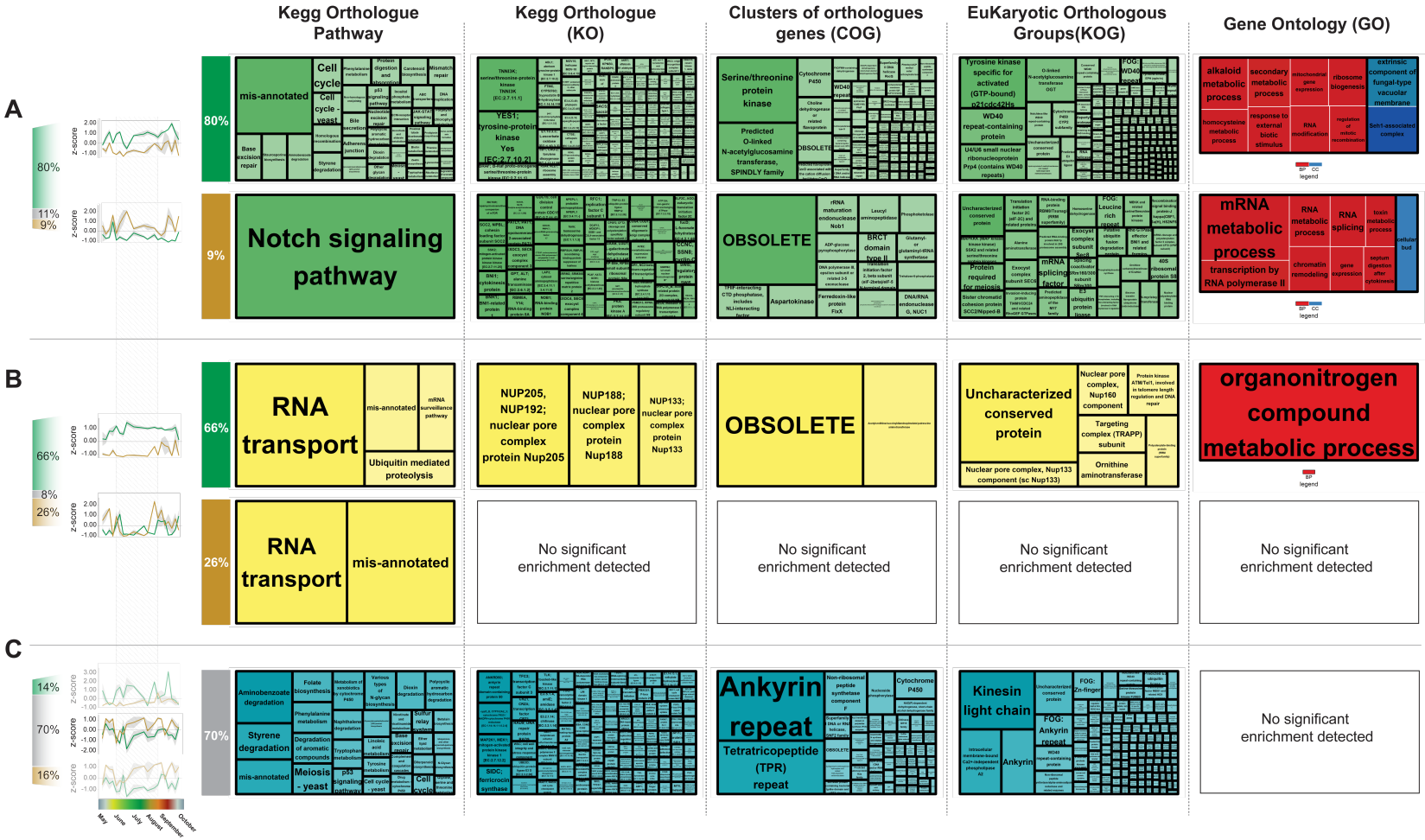


**Fig. S4. Functional enrichment analysis of the three fungal species with the highest RNA-Seq read assignment.** For the three fungal species **(A)** *Piloderma olivaceum* **(B)** *Cortinarius glaucopus* **(C)** *Cenococcum geophilum*, functional enrichment tests covering five categories (KEGG pathways, KO, COG, KOG, and GO) was determined using a Fisher exact test (adjusted $P$<0.05) and the results were represented in the form of treemaps. For each treemap, the statistical significance of enrichment is displayed in relation to the size and color-intensity of the box the function is displayed in; e.g. functions with greater significance of enrichment are in larger boxes, while functions with lower significance of enrichment are in smaller boxes. The result and figure can be recreated using the Boreal Rhizospheric Atlas (BRA) online tool (https://www.boreal-atlas.info/) to allow full exploration. For both *Piloderma olivaceum* and *Cortinarius glaucopus*, functional enrichment analysis was carried out on those genes that were

significantly differentially expressed between NL and NE conditions, as these accounted for the majority of genes in these two species (89% and 92%, respectively). For *Cenococcum geophilum*, the majority of genes were not differentially expressed between treatments (70%), thus functional enrichment analysis was carried out on this cohort of genes.

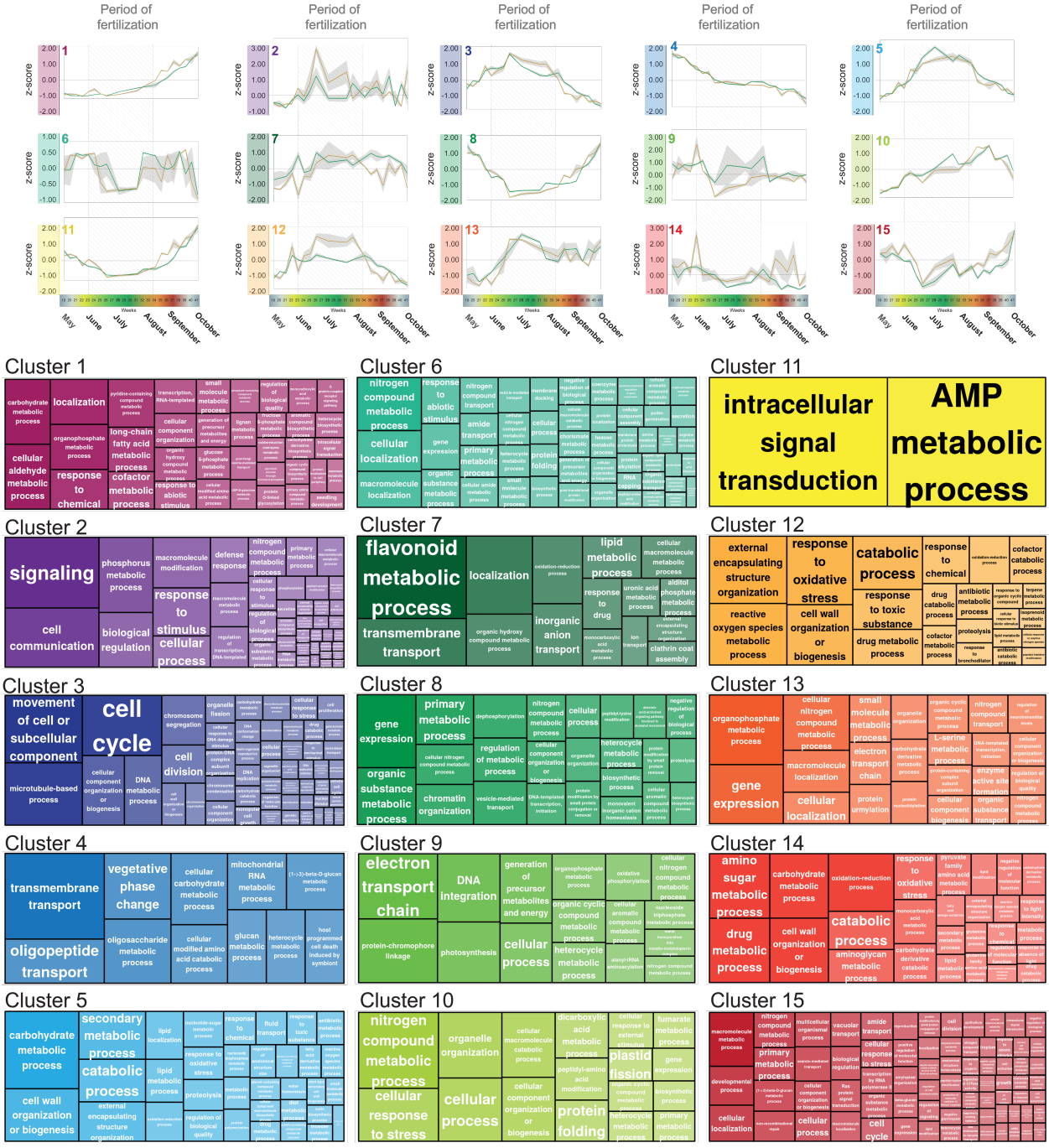


**Fig. S5. Functional enrichment analysis of a Norway spruce fine root co-expression network, sampled from nutrient limited and nutrient enriched plots over a growing season.** This co-expression network (shown in Fig. 3B) is composed exclusively of Norway spruce genes. Significantly enriched functional categories have been listed in the form of treemaps (adjusted $P$<0.05 in all cases; Fisher exact test). For each treemap, the statistical significance of enrichment is displayed in relation to the size and color-intensity of the box the function is displayed in; e.g. functions with greater significance of enrichment

are in larger boxes, while functions with lower significance of enrichment are in smaller boxes. The result and figure can be recreated using the Boreal Rhizospheric Atlas (BRA) online tool (https://www.boreal-atlas.info/) to allow full exploration.

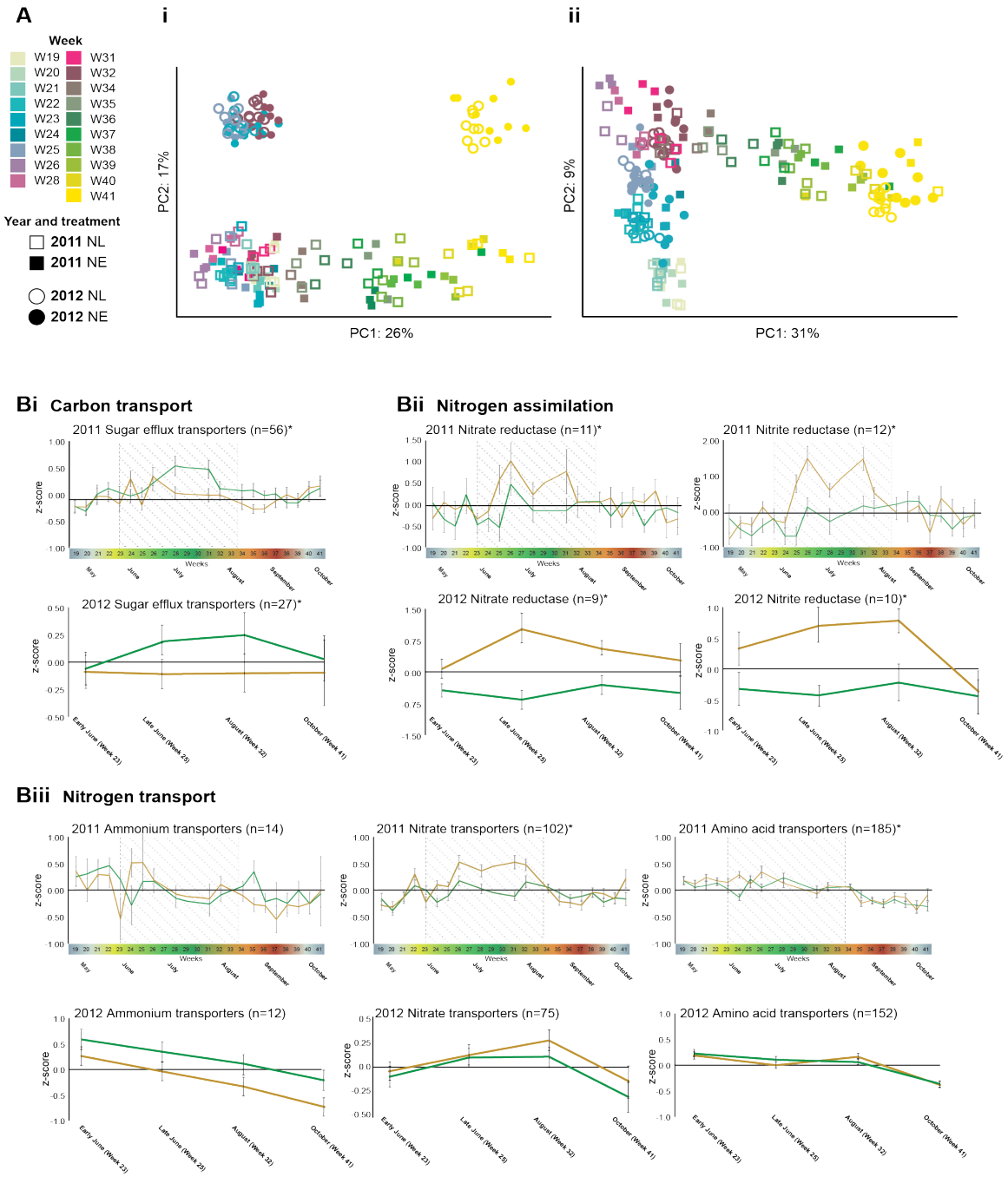


**Fig. S6. Comparison of Norway spruce transcriptomes from samples collected in 2011 and 2012.** **(Ai)** PCA of Norway spruce fine root transcriptomes from samples collected across a seasonal time courses in both nutrient limited and nutrient enriched conditions in both 2011 and 2012, and **(Aii)** when year effect has been removed. **(B)** Expression of functions associated with **(i)** carbon transport, **(ii)** nitrogen assimilation, and **(iii)** nitrogen transport; from samples collected across a seasonal time courses in both nutrient limited and nutrient enriched conditions in both 2011 and 2012. An * indicates significant ($P$<0.01) difference in transcript abundance using a two-tailed Wilcoxon Signed-Rank Test. Error bars indicate standard error.

**A**

| Norway spruce Network Module | *Piloderma olivaceum* Network Module | NL Correlation | NE Correlation |
|---|---|---|---|
| 10 | 2:1:5 | 0.19 | 0.73 |
| 10 | 2:1:3 | 0.16 | 0.70 |
| 14 | 1:3:4 | -0.72 | -0.09 |
| 15i | 1:1:1 | 0.75 | 0.40 |
| 20 | 1:4:1 | -0.74 | -0.38 |
| 20 | 1:1:2 | -0.70 | -0.34 |
| 20 | 1:4:4 | -0.74 | -0.33 |
| 20 | 1:4:3 | -0.77 | -0.33 |
| 27 | 2:4:4 | -0.73 | -0.24 |
| 27 | 2:4:2 | -0.70 | -0.21 |
| 27 | 2:4:1 | -0.71 | -0.21 |
| 27 | 2:4:5 | -0.71 | -0.18 |
| 30 | 1:3:1 | -0.73 | 0.08 |
| 30 | 1:3:5 | -0.80 | 0.07 |
| 33 | 1:4:5 | -0.75 | -0.26 |
| 33 | 2:1:5 | -0.73 | -0.24 |
| 33 | 2:1:2 | -0.70 | -0.21 |
| 33 | 2:1:1 | -0.71 | -0.20 |
| 33 | 2:1:3 | -0.71 | -0.19 |

**B**

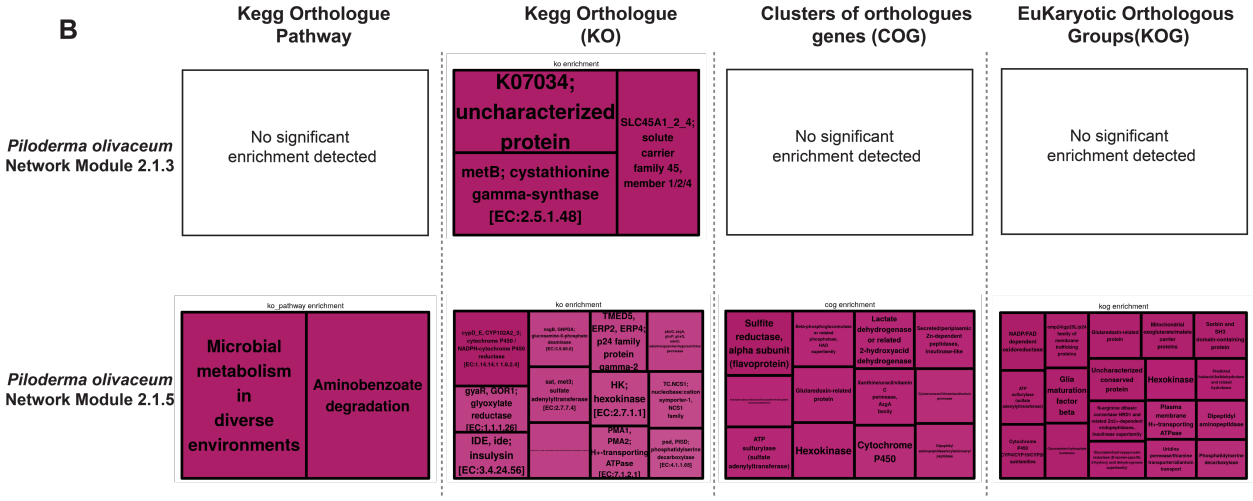


**Fig. S7. Functional enrichment analysis of *Piloderma olivaceum* network modules. (A)** Table of network module combinations, between Norway spruce and *Piloderma olivaceum*. **(B)** Significantly enriched functional categories of specific network modules mentioned in the text have been listed in the form of treemaps (adjusted $P<0.05$ in all cases; Fisher exact test). For each treemap, the statistical significance of enrichment is displayed in relation to the size and color-intensity of the box the function is displayed in; e.g. functions with greater significance of enrichment are in larger boxes, while functions with lower significance of enrichment are in smaller boxes. The result and figure can be recreated using the Boreal Rhizospheric Atlas (BRA) online tool (https://www.boreal-atlas.info/) to allow full exploration.

**A**

| Norway spruce Network Module | *Cenococcum geophilum* Network Module | NL Correlation | NE Correlation | |
|---|---|---|---|---|
| 5i | 14 | 0.89 | 0.86 | |
| 2 | 4 | 0.81 | 0.76 | |
| 30i | 14 | 0.80 | 0.73 | |
| 7 | 14 | 0.76 | 0.84 | |
| 21 | 14 | 0.74 | 0.79 | |
| 1 | 14 | 0.74 | 0.74 | |
| 17i | 14 | 0.71 | 0.88 | |
| 7i | 14 | -0.71 | -0.83 | *Cenococcum geophilum* Network Module 4 |
| 29 | 14 | -0.72 | -0.80 | |
| 1i | 14 | -0.74 | -0.72 | |
| 25 | 14 | -0.75 | -0.72 | |
| 23 | 14 | -0.76 | -0.80 | |
| 21i | 14 | -0.79 | -0.74 | |
| 18i | 14 | -0.84 | -0.81 | |
| 30 | 14 | -0.85 | -0.86 | |
| 5 | 14 | -0.89 | -0.85 | |
| 29 | 21 | 0.06 | 0.81 | |
| 16i | 14 | 0.58 | 0.81 | |
| 13i | 14 | -0.47 | 0.79 | |
| 7i | 21 | 0.00 | 0.76 | |
| 14i | 14 | 0.42 | 0.76 | |
| 25i | 28 | 0.26 | 0.75 | |
| 9i | 14 | 0.66 | 0.75 | |
| 14 | 21 | 0.10 | 0.74 | *Cenococcum geophilum* Network Module 14 |
| 5 | 21 | -0.10 | 0.74 | |
| 30i | 28 | 0.44 | 0.74 | |
| 5i | 28 | 0.38 | 0.73 | |
| 25i | 14 | 0.47 | 0.73 | |
| 26i | 28 | 0.49 | 0.73 | |
| 15i | 3 | 0.14 | 0.73 | |
| 9i | 28 | 0.26 | 0.72 | |
| 30i | 2 | 0.11 | 0.72 | |
| 21i | 21 | -0.35 | 0.71 | |
| 30 | 21 | -0.06 | 0.71 | |
| 12i | 4 | 0.48 | 0.71 | |
| 21 | 28 | 0.41 | 0.71 | |
| 18 | 21 | -0.10 | -0.70 | |
| 25 | 28 | -0.07 | -0.70 | |
| 26i | 21 | 0.20 | -0.70 | |
| 15 | 3 | -0.25 | -0.70 | |
| 26 | 28 | -0.15 | -0.71 | |
| 17 | 28 | -0.17 | -0.72 | |
| 11 | 14 | -0.54 | -0.72 | |
| 30 | 28 | -0.28 | -0.73 | |
| 18 | 29 | 0.09 | -0.73 | |
| 7 | 21 | 0.00 | -0.74 | |
| 14 | 14 | -0.55 | -0.75 | |
| 16 | 14 | -0.62 | -0.75 | |
| 23 | 28 | -0.38 | -0.76 | |
| 18i | 28 | -0.31 | -0.77 | |
| 16i | 21 | 0.12 | -0.78 | |
| 17 | 14 | -0.57 | -0.78 | |
| 25i | 21 | -0.06 | -0.79 | |
| 9i | 21 | 0.03 | -0.79 | |
| 21 | 21 | -0.03 | -0.79 | |
| 26 | 14 | -0.44 | -0.84 | |
| 23i | 14 | 0.77 | 0.60 | *Cenococcum geophilum* Network Module 28 |
| 8 | 4 | -0.73 | -0.36 | |

**B**

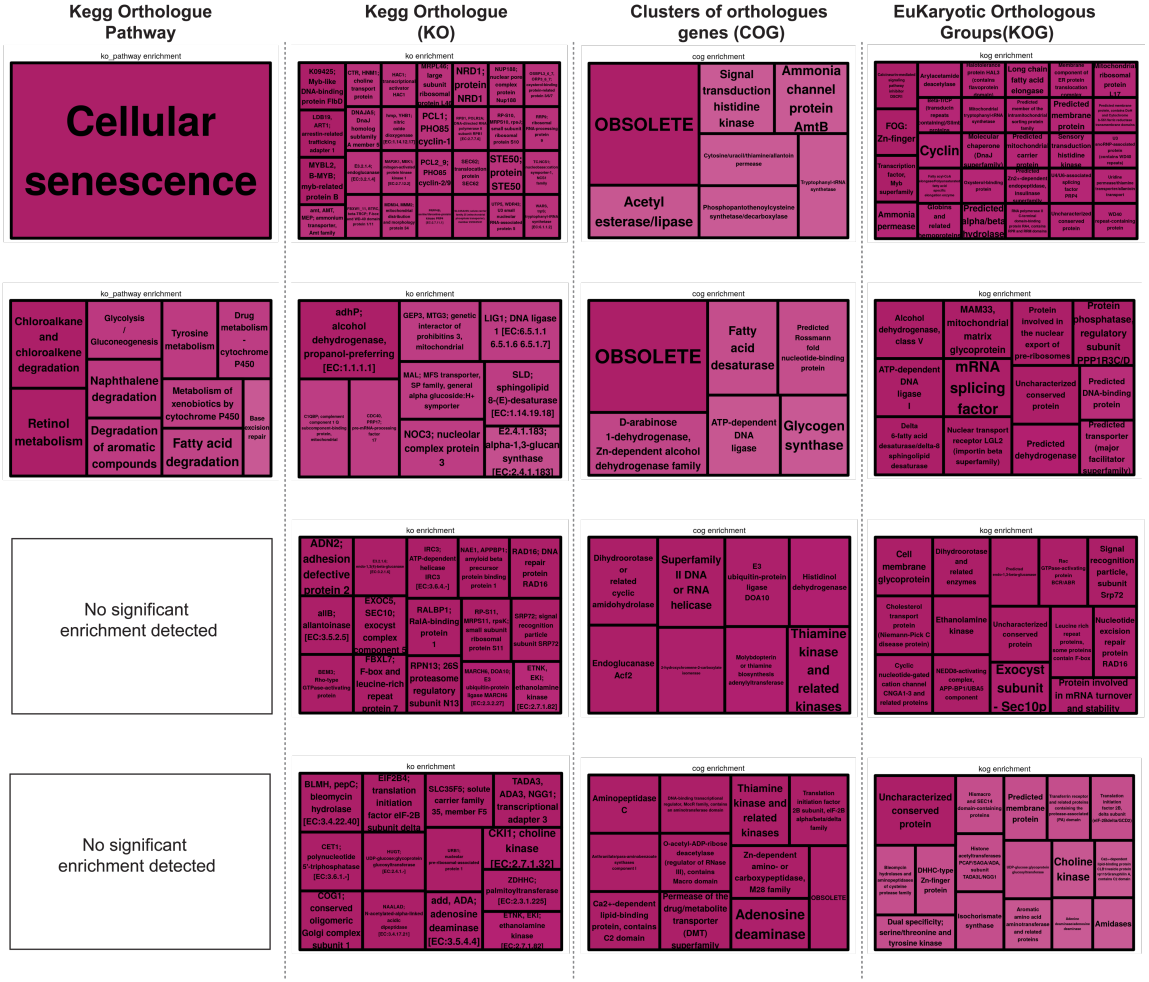


**Fig. S8. Functional enrichment analysis of *Cenococcum geophilum* network modules. (A)** Table of network module combinations, between Norway spruce and *Cenococcum geophilum*. **(B)** Significantly enriched functional categories of specific network modules mentioned in the text have been listed in the form of treemaps (adjusted $P<0.05$ in all cases; Fisher exact test). For each treemap, the statistical significance of enrichment is displayed in relation to the size and color-intensity of the box the function is displayed in; e.g. functions with greater significance of enrichment are

in larger boxes, while functions with lower significance of enrichment are in smaller boxes. The result and figure can be recreated using the Boreal Rhizospheric Atlas (BRA) online tool (https://www.boreal-atlas.info/) to allow full exploration.

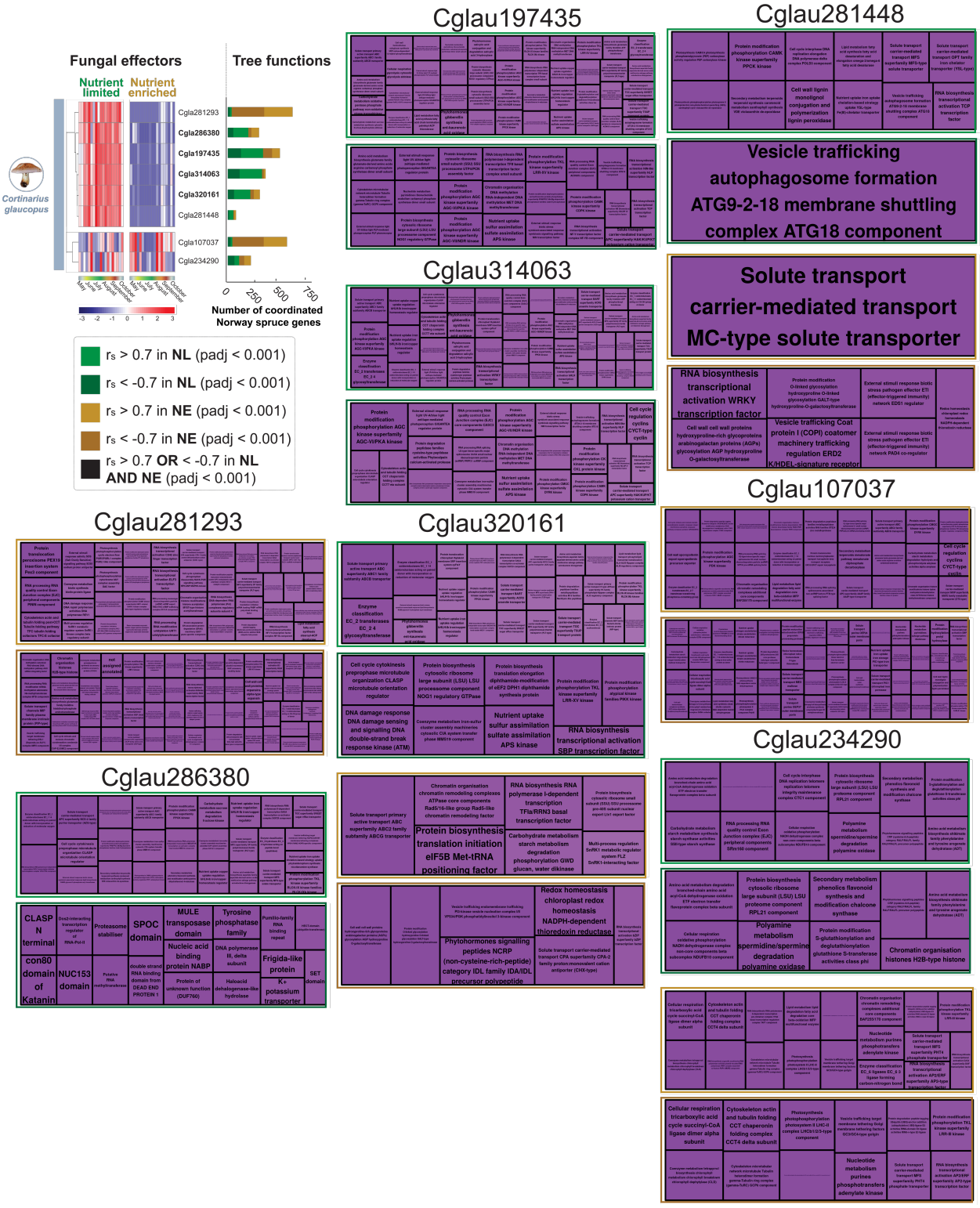


**Fig. S9. Coordination of predicted *Cortinarius glaucopus* effectors and Norway spruce transcriptome in nutrient limited and nutrient enriched samples over a growing season.** Spearman rank correlation was used to measure the coordination between an individual predicted fungal effector and

the complete Norway spruce transcriptome. In both cases, to be considered “coordinated” the correlation between two network modules or between a fungal effector and a Norway spruce transcript had to satisfy the following: $r_s$ (> 0.7 or <-0.7) and adjusted *P* thresholds (<0.001). This was carried out in NL and NE conditions in isolation, to establish if coordination was observed in NL, NE, or BOTH conditions. Functional enrichment of Norway spruce transcripts coordinated with individual fungal effectors was carried out using the Boreal Rhizospheric Atlas (BRA) online tool. Example functional enrichment outputs for specific fungal effector-coordinated Norway spruce transcripts have been provided. For each treemap, the statistical significance of enrichment is displayed in relation to the size and color-intensity of the box the function is displayed in; e.g. functions with greater significance of enrichment are in larger boxes, while functions with lower significance of enrichment are in smaller boxes. The result and figure can be recreated using the BRA online tool (https://www.boreal-atlas.info/) to allow full exploration.

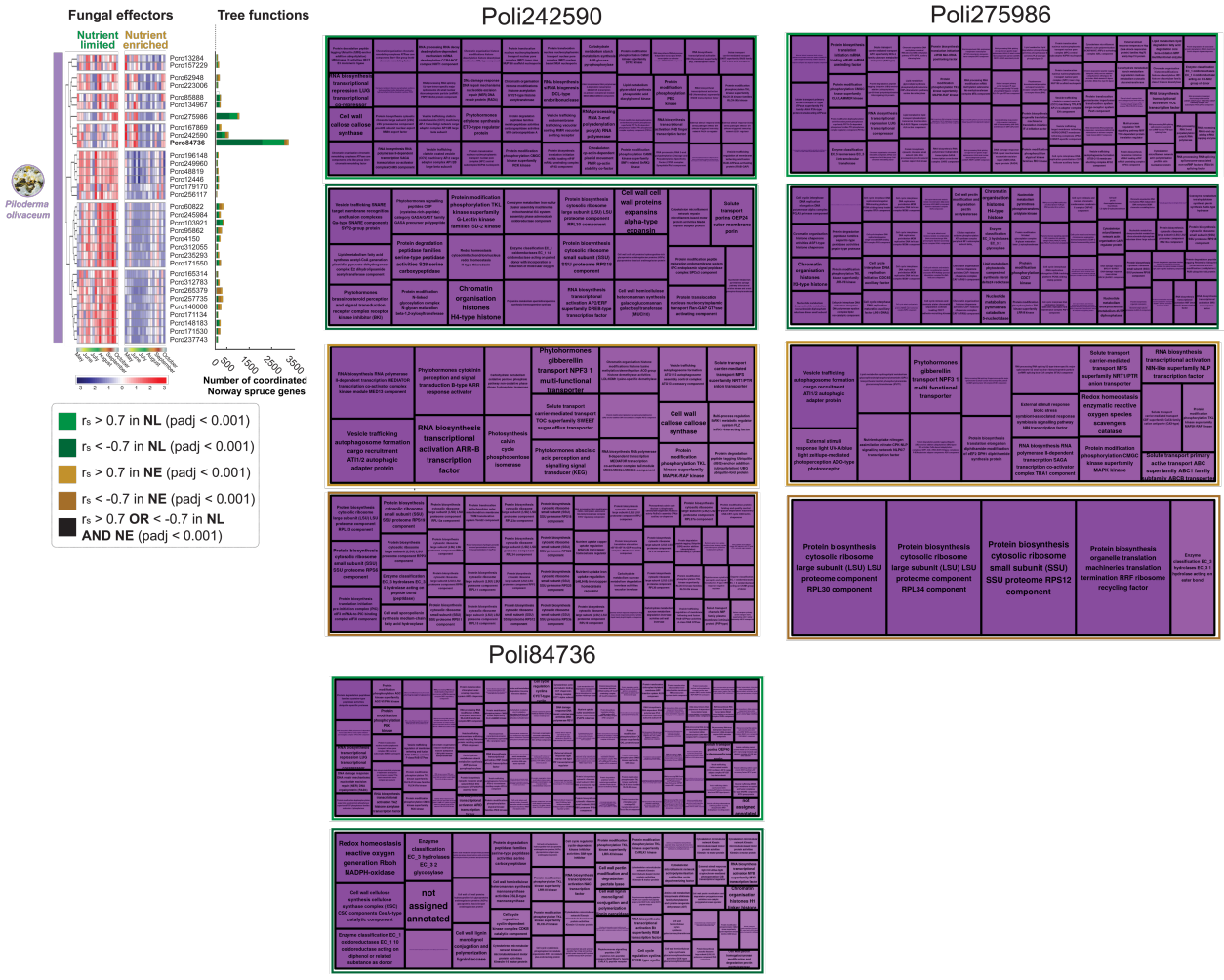


**Fig. S10. Coordination of predicted *Piloderma olivaceum* effectors and Norway spruce transcriptome in nutrient limited and nutrient enriched samples over a growing season.** Spearman rank correlation was used to measure the coordination between an individual predicted fungal effector and the complete Norway Spruce transcriptome. In both cases, to be considered "coordinated" the correlation between two network modules or between a fungal effector and a Norway spruce transcript had to satisfy the following: $r_s$ (> 0.7 or <-0.7) and adjusted *P* thresholds (<0.001). This was carried out in NL and NE conditions in isolation, to establish if coordination was observed in NL, NE, or BOTH conditions. Functional enrichment of Norway spruce transcripts coordinated with individual fungal effectors was carried out using the Boreal Rhizospheric Atlas (BRA) online tool. Example functional enrichment outputs for specific fungal effector coordinated Norway spruce transcripts have been provided. For each treemap, the statistical significance of enrichment is displayed in relation to the size and color-intensity of the box the function is displayed in; e.g. functions with greater significance of enrichment are in larger boxes, while functions with

lower significance of enrichment are in smaller boxes. The result and figure can be recreated using the BRA online tool (https://www.boreal-atlas.info/) to allow full exploration.

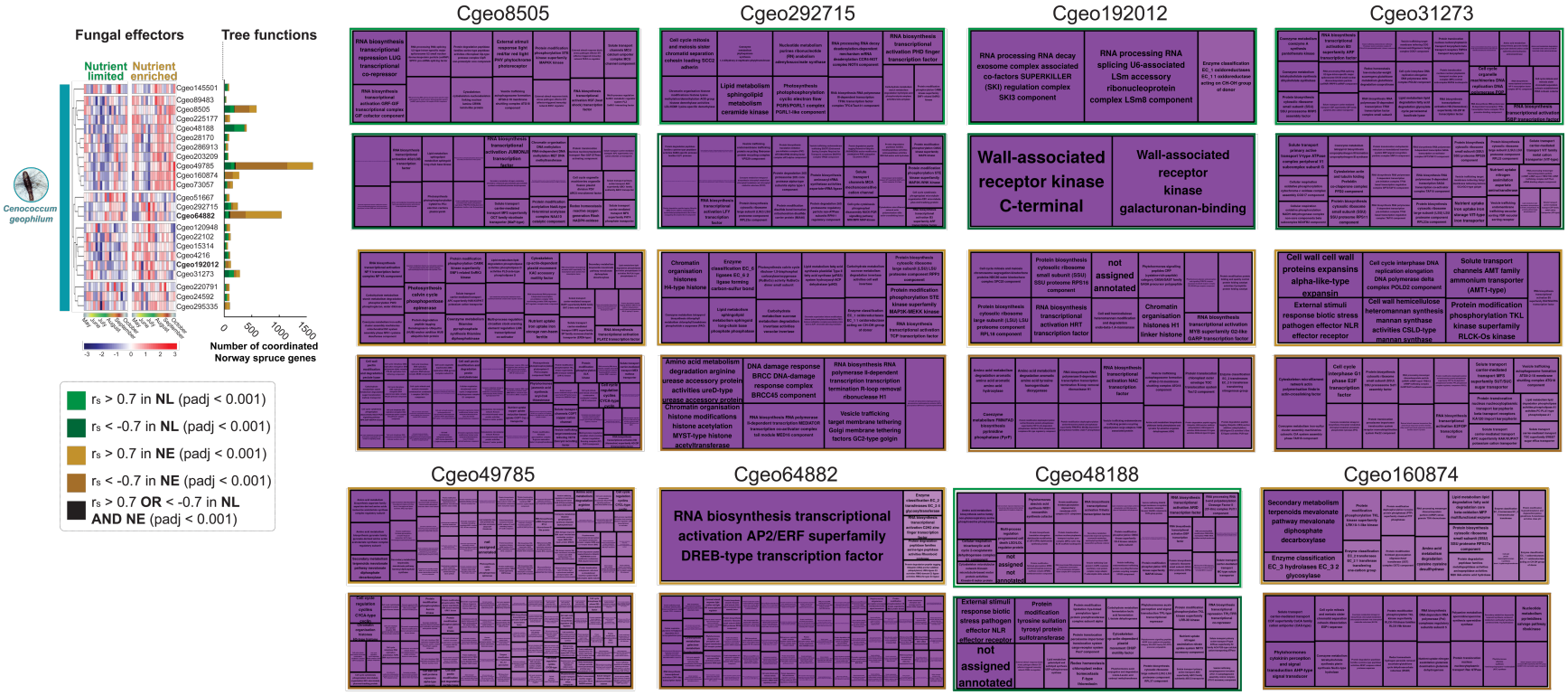


**Fig. S11 Coordination of predicted *Cenococcum geophilum* effectors and Norway spruce transcriptome in nutrient limited and nutrient enriched samples over a growing season.** Spearman rank correlation was used to measure the coordination between an individual predicted fungal effector and the complete Norway spruce transcriptome. In both cases, to be considered "coordinated" the correlation between two network modules or between a fungal effector and a Norway spruce transcript had to satisfy the following: $r_s$ (> 0.7 or <-0.7) and adjusted *P* thresholds (<0.001). This was carried out in NL and NE conditions in isolation, to establish if coordination was observed in NL, NE, or BOTH conditions. Functional enrichment of Norway spruce transcripts coordinated with individual fungal effectors was carried out using the Boreal Rhizospheric Atlas (BRA) online tool. Example functional enrichment outputs for specific fungal effector-coordinated Norway spruce transcripts have been provided. For each treemap, the statistical significance of enrichment is displayed in relation to the size and color-intensity of the box the function is displayed

in; e.g. functions with greater significance of enrichment are in larger boxes, while functions with lower significance of enrichment are in smaller boxes. The result and figure can be recreated using the BRA online tool (https://www.boreal-atlas.info/) to allow full exploration.

**References**


1. J. C. Haas *et al.*, Microbial community response to growing season and plant nutrient optimisation in a boreal Norway spruce forest. *Soil Biol Biochem* **125**, 197-209 (2018).
2. S. Linder, Foliar Analysis for Detecting and Correcting Nutrient Imbalances in Norway Spruce. *Ecological Bulletins* **44**, 178-190 (1995).
3. S. R. Law *et al.*, Data from "Metatranscriptomics captures dynamic shifts in mycorrhizal coordination in boreal forests". European Nucleotide Archive, [submitted 2020] https://www.ebi.ac.uk/ena/browser/text-search?query=PRJEB35805.
4. A. N. Schneider *et al.*, Comparative Fungal Community Analyses Using Metatranscriptomics and Internal Transcribed Spacer Amplicon Sequencing from Norway Spruce. *mSystems* **6** (2021).
5. E. Kopylova, L. Noe, H. Touzet, SortMeRNA: fast and accurate filtering of ribosomal RNAs in metatranscriptomic data. *Bioinformatics* **28**, 3211-3217 (2012).
6. A. M. Bolger, M. Lohse, B. Usadel, Trimmomatic: a flexible trimmer for Illumina sequence data. *Bioinformatics* **30**, 2114-2120 (2014).
7. R. Patro, G. Duggal, M. I. Love, R. A. Irizarry, C. Kingsford, Salmon provides fast and bias-aware quantification of transcript expression. *Nat Methods* **14**, 417-419 (2017).
8. C. Luo, R. L. Rodriguez, K. T. Konstantinidis, MyTaxa: an advanced taxonomic classifier for genomic and metagenomic sequences. *Nucleic Acids Res* **42**, e73 (2014).
9. J. Alneberg *et al.*, BARM and BalticMicrobeDB, a reference metagenome and interface to meta-omic data for the Baltic Sea. *Sci Data* **5**, 180146 (2018).
10. C. P. Cantalapiedra, A. Hernandez-Plaza, I. Letunic, P. Bork, J. Huerta-Cepas, eggNOG-mapper v2: Functional Annotation, Orthology Assignments, and Domain Prediction at the Metagenomic Scale. *Mol Biol Evol* 10.1093/molbev/msab293 (2021).
11. K. R. Moon *et al.*, Visualizing structure and transitions in high-dimensional biological data. *Nat Biotechnol* **37**, 1482-1492 (2019).
12. M. I. Love, W. Huber, S. Anders, Moderated estimation of fold change and dispersion for RNA-seq data with DESeq2. *Genome Biol* **15**, 550 (2014).
13. B. Schiffthaler, A. R. Serrano, N. Street, N. Delhomme, Seidr: a gene meta-network calculation toolkit. *bioRxiv* 10.1101/250696.
14. R. M, A. D, B. C, The map equation. *Eur. Phys. J. Spec. Top.* **178**, 13–23 (2009).
15. B. D. Sigurdsson, J. L. Medhurst, G. Wallin, O. Eggertsson, S. Linder, Growth of mature boreal Norway spruce was not affected by elevated [CO2] and/or air temperature unless nutrient availability was improved. *Tree Physiol* **33**, 1192-1205 (2013).
16. H. Majdi, P. Andersson, Fine Root Production and Turnover in a Norway Spruce Stand in Northern Sweden: Effects of Nitrogen and Water Manipulation. *Ecosystems* **8**, 191-199 (2005).
17. J. Leppälammi-Kujansuu *et al.*, Effects of long-term temperature and nutrient manipulation on Norway spruce fine roots and mycelia production. *Plant Soil* **366**, 287–303 (2013).
18. J. J. Almagro Armenteros *et al.*, SignalP 5.0 improves signal peptide predictions using deep neural networks. *Nat Biotechnol* **37**, 420-423 (2019).
19. L. Kall, A. Krogh, E. L. Sonnhammer, Advantages of combined transmembrane topology and signal peptide prediction--the Phobius web server. *Nucleic Acids Res* **35**, W429-432 (2007).

20. J. Sperschneider, P. N. Dodds, D. M. Gardiner, K. B. Singh, J. M. Taylor, Improved prediction of fungal effector proteins from secretomes with EffectorP 2.0. *Mol Plant Pathol* **19**, 2094-2110 (2018).
21. M. Hall (2008) Effects of future climate on carbon assimilation of boreal Norway spruce. in *Department of Plant and Environmental Sciences, Faculty of Science* (University of Gothenburg).
22. P. Olsson, S. Linder, R. Giesler, P. Hogberg, Fertilization of boreal forest reduces both autotrophic and heterotrophic soil respiration. *Global Change Biol* **11**, 1745-1753 (2005).